INSTITUTE OF PHYSICS PUBLISHING and INTERNATIONAL ATOMIC ENERGY AGENCY NUCLEAR FUSION

Nucl. Fusion **46** (2006) S22–S28 doi:10.1088/0029-5515/46/3/S04

Progress towards steady state on NSTX

D.A. Gates[1], C. Kessel[1], J. Menard[1], G. Taylor[1], J.R. Wilson[1], M.G. Bell[1], R.E. Bell[1], S. Bernabei[1], J. Bialek[2], T. Biewer[1], W. Blanchard[1], J. Boedo[3], C. Bush[4], M.D. Carter[4], W. Choe[5], N. Crocker[6], D.S. Darrow[1], W. Davis[1], L. Delgado-Aparicio[7], S. Diem[1], J. Ferron[8], A. Field[9], J. Foley[1], E.D. Fredrickson[1], T. Gibney[1], R. Harvey[10], R.E. Hatcher[1], W. Heidbrink[11], K. Hill[1], J.C. Hosea[1], T.R. Jarboe[12], D.W. Johnson[1], R. Kaita[1], S. Kaye[1], S. Kubota[6], H.W. Kugel[1], J. Lawson[1], B.P. LeBlanc[1], K.C. Lee[13], F. Levinton[14], R. Maingi[4], J. Manickam[1], R. Maqueda[14], R. Marsala[1], D. Mastrovito[1], T.K. Mau[3], S.S. Medley[1], H. Meyer[9], D.R. Mikkelsen[1], D. Mueller[1], T. Munsat[15], B.A. Nelson[12], C. Neumeyer[1], N. Nishino[16], M. Ono[1], H. Park[1], W. Park[1], S. Paul[1], T. Peebles[6], M. Peng[4], C. Phillips[1], A. Pigarov[3], R. Pinsker[8], A. Ram[17], S. Ramakrishnan[1], R. Raman[12], D. Rasmussen[4], M. Redi[1], M. Rensink[18], G. Rewoldt[1], J. Robinson[1], P. Roney[1], L. Roquemore[1], E. Ruskov[11], P. Ryan[4], S.A. Sabbagh[2], H. Schneider[1], C.H. Skinner[1], D.R. Smith[1], A. Sontag[2], V. Soukhanovskii[18], T. Stevenson[1], D. Stotler[1], B. Stratton[1], D. Stutman[7], D. Swain[4], E. Synakowski[1], Y. Takase[19], K. Tritz[7], A. von Halle[1], M. Wade[4], R. White[1], J. Wilgen[4], M. Williams[1], W. Zhu[2], S.J. Zweben[1], R. Akers[9], P. Beiersdorfer[18], R. Betti[20], T. Bigelow[4]

[1] Princeton Plasma Physics Laboratory, Princeton University, Princeton, NJ 08543, USA
[2] Department of Applied Physics, Columbia University, New York City, NY, USA
[3] University of California, San Diego, CA, USA
[4] Oak Ridge National Laboratory, Oak Ridge, TN, USA
[5] Korea Advanced Institute of Science and Technology, Taejon, Korea
[6] University of California, Los Angeles, CA, USA
[7] Johns Hopkins University, Baltimore, MD, USA
[8] General Atomics, San Diego, CA, USA
[9] Euratom-UKAEA Fusion Associates, Abingdon, Oxfordshire, UK
[10] CompX, Del Mar, CA, USA
[11] University of California, Irvine, CA, USA
[12] University of Washington, Seattle, WA, USA
[13] University of California, Davis, CA, USA
[14] Nova Photonics, Princeton, NJ, USA
[15] University of Colorado, Boulder, CO, USA
[16] Hiroshima University, Hiroshima, Japan
[17] Massachusetts Institute of Technology, Cambridge, MA, USA
[18] Lawrence Livermore National Laboratory, Livermore, CA, USA
[19] Tokyo University, Tokyo, Japan
[20] University of Rochester, Rochester, NY, USA

Received 10 March 2005, accepted for publication 30 December 2005
Published 25 January 2006
Online at stacks.iop.org/NF/46/S22

Abstract
In order to reduce recirculating power fraction to acceptable levels, the spherical torus concept relies on the simultaneous achievement of high toroidal β and high bootstrap fraction in steady state. In the last year, as a result of plasma control system improvements, the achievable plasma elongation on NSTX has been raised from $\kappa \sim 2.1$ to $\kappa \sim 2.6$—approximately a 25% increase. This increase in elongation has led to a substantial increase

in the toroidal β for long pulse discharges. The increase in β is associated with an increase in plasma current at nearly fixed poloidal β, which enables higher β_t with nearly constant bootstrap fraction. As a result, for the first time in a spherical torus, a discharge with a plasma current of 1 MA has been sustained for 1 s (0.8 s current flat-top). Data are presented from NSTX correlating the increase in performance with increased plasma shaping capability. In addition to improved shaping, H-modes induced during the current ramp phase of the plasma discharge have been used to reduce flux consumption and to delay the onset of MHD instabilities. Based on these results, a modelled integrated scenario, which has 100% non-inductive current drive with very high toroidal β, will also be discussed. The NSTX poloidal field coils are currently being modified to produce the plasma shape which is required for this scenario, which requires high triangularity ($\delta \sim 0.8$) at elevated elongation ($\kappa \sim 2.5$). The other main requirement of steady state on NSTX is the ability to drive a fraction of the total plasma current with RF waves. The results of high harmonic fast wave heating and current drive studies as well as electron Bernstein wave emission studies will be presented.

PACS numbers: 52.55.Fa, 52.55.Dy, 52.55.Rk

1. Introduction

The spherical torus concept [1] (i.e. a tokamak with $R/a \sim 1$) is an extension of the same reasoning that leads to the steady-state advanced tokamak concept. Using the bootstrap current and the external non-inductive current drive to sustain a tokamak in steady state is an immediate precursor to the concept of changing the geometry of the torus to optimize bootstrap current and minimize the need for a transformer to drive current inductively. The spherical torus concept takes the extreme step of eliminating the transformer and maximizing toroidal field utilization by reducing the physical size of the toroidal field coil to engineering limits. This extreme geometry also leads to challenges. In particular, as the aspect ratio is reduced, the ability to shield the centre column of the toroidal coil is reduced. In the low aspect ratio limit, it becomes impossible to use known superconducting materials to build a toroidal field coil for a reactor due to nuclear heating. This lack of shielding then requires low aspect ratio devices to employ conventional conductors, which in turn forces the device to operate at very high toroidal β so as to minimize the recirculating power fraction. Fortunately, the achievable β is increased at low aspect ratio. In addition to the higher β limits, the achievable elongation is also higher at low aspect ratio. This is important since the bootstrap fraction at fixed normalized $\beta(\equiv\beta_N)$ and $q^\star$ scales like $\sim 1+\kappa^2$ (where $\beta_N \equiv \beta_t * aB_t/I_p$, with $\beta_t \equiv 2\mu_0\langle P\rangle/B_t^2$ and $q^\star \equiv \pi a^2(1+\kappa^2)B_t/(\mu_0 R I_p)$).

The National Spherical Torus Experiment [2] is a low aspect ratio torus ($A = R/a \sim 1.3$, where A is the aspect ratio, R is the major radius of the torus and a is the minor radius of the torus). NSTX has previously achieved $\beta_t \sim 35\%$ and non-inductive current fractions of $\sim$60% [3], albeit not simultaneously. Recently, the operating regime of the device has been expanded to help explore the high κ operating space that has been identified as the most attractive one for the ST concept. The consequence of this expanded operating regime was a substantial improvement in the achievable β_t in long pulse discharges, as expected by MHD stability theory and neoclassical theory. The details of the observed improvement will be discussed in section 2. In addition to the improved shaping capability, H-modes were triggered early in the current ramp, which reduces flux consumption as described in section 3. Integrated scenario modelling indicates that a 100% non-inductive current drive at $\beta_t \sim 40\%$ is possible on NSTX. Results from these calculations as well as machine modifications in support of developing this scenario will be presented in section 4. NSTX is also investigating external non-inductive current drive options. In particular, NSTX has successfully driven current using the high harmonic fast waves (HHFWs). Results from both heating and current drive experiments will be discussed in section 5. Future plans include using electron Bernstein waves (EBWs) for external current drive and electron heating. Results from EBW emission experiments, which were carried out in order to determine the feasibility of these plans, will also be discussed in section 5.

2. Widened operating regime

The improvement in operating regime for NSTX was achieved primarily by improving plasma control capabilities. In particular, the digital control system on NSTX was improved to reduce control latency. The control latency (defined as the propagation time of a perturbation through the control system) is an important parameter for determining the maximum gain in a control loop. The average latency in the NSTX control system was reduced by a factor of 4 to $\sim$0.75 ms via hardware upgrades and software optimization. In addition to the improvements in control latency, an analog measurement of the vertical voltage difference was added to improve the fidelity of the derivative term in the digital vertical position control loop. This led to an increase in the sustainable plasma elongation from a previous high of $\kappa \sim 2.1$ to a new high $\kappa \sim 2.6$. Shown in figure 1 is a plot of the achieved plasma elongation as determined by the EFIT equilibrium reconstruction code [4,5] versus the normalized internal inductance, l_i, also determined by EFIT. The growth rate of the $n = 0$ vertical instability increases with increasing l_i and κ. The upper boundary of the κ versus l_i operating space will correspond (roughly) to a curve of constant vertical growth rate. As can be seen in figure 1 the increase in κ is $\sim$20% at fixed l_i.

The improvement in κ has led to a corresponding increase in the β_t attainable for long pulse discharges. Time histories of the plasma current and β_t for the best discharge (i.e. longest pulse) from 2002 and 2004 is shown in figure 2. As can be seen from the figure, the plasma current has been increased by

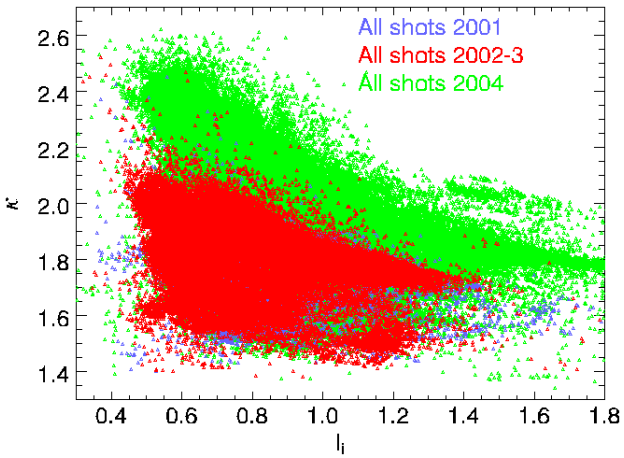

Figure 1. Plot of the vertical stability space of the entire NSTX database, plotting plasma elongation (κ) versus normalized internal inductance (l_i). Each point represents a single timeslice of an NSTX plasma discharge. Values are calculated using the EFIT ideal MHD equilibrium reconstruction code.

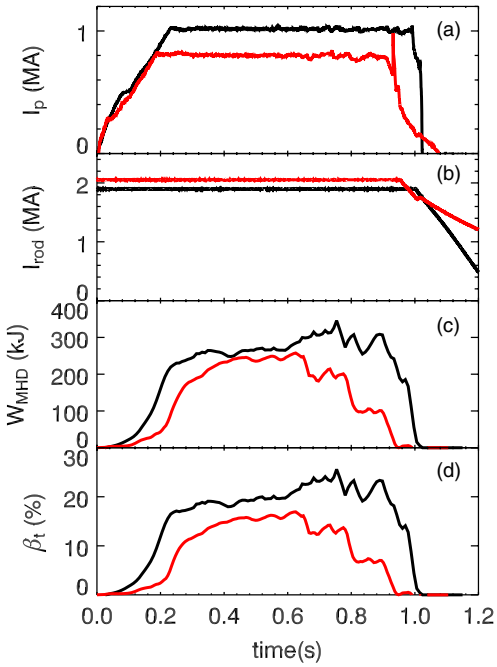

Figure 2. Comparison of the 'best' shots from 2004 (after control improvements, black) and from 2002 (before control improvements, red). Shown in each panel are (*a*) plasma current (MA), (*b*) total current in the toroidal field central rod (MA), (*c*) the stored kinetic energy in the plasma (from EFIT) and (*d*) β_t (from EFIT) all versus time. Plasma current is increased by 25%, TF current is reduced by 10% and β_t is correspondingly increased by a factor of two (pulse averaged).

25%, the toroidal field current has been decreased by ~10% and the pulse length has increased. Accordingly, the peak β_t has been increased by ~50%. Additionally, the plasma stored energy does not drop until the end of the current flat-top which further increases the pulse-averaged β_t. The change in plasma cross-section for the plasma discharges shown in figure 2 is shown in figure 3. The red boundary in figure 3 is the earlier lower κ, lower β_t discharge. The time history of the pressure driven and neutral beam driven current fractions as calculated

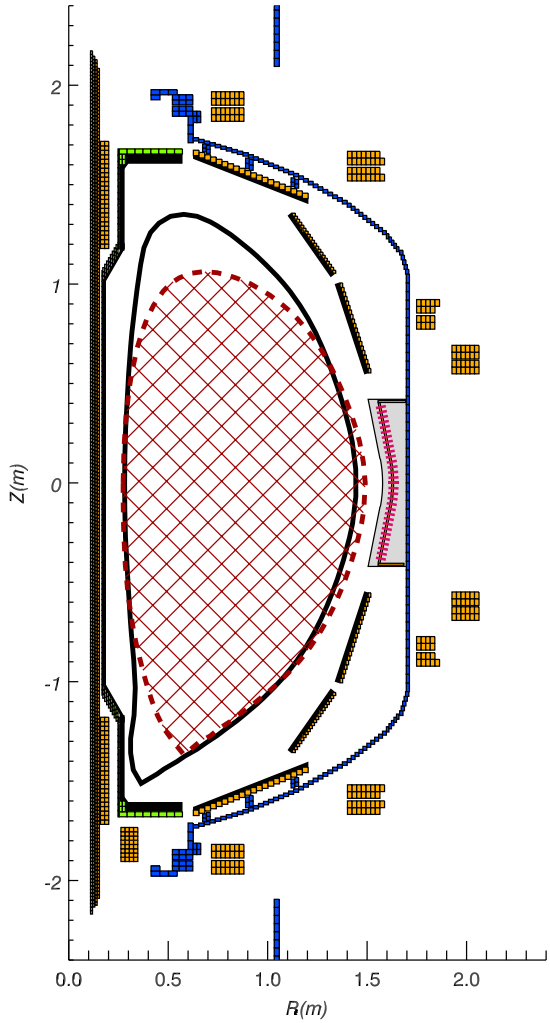

Figure 3. Overlay of the boundaries of the plasma discharges shown in figure 2. Plasma elongation is $\kappa \sim 2.1$ for shot 109063 (dashed red) and $\kappa \sim 2.5$ for shot 112581 (solid black).

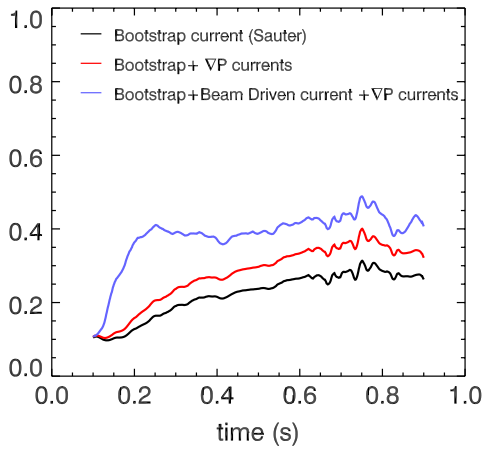

Figure 4. Non-inductive current fractions for shot 112581 as calculated by the TRANSP code.

by the TRANSP code [6] is shown in figure 4 for the higher current discharge from figure 2.

To help quantify the connection between the increase in plasma elongation and the observed improvement in

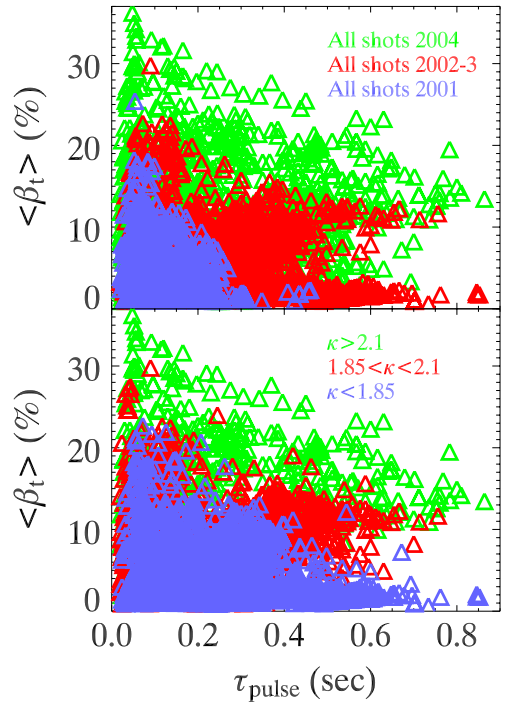

Figure 5. Plot of the pulse averaged β_t versus the pulse length over which β_t was averaged. The pulse length is determined from the plasma current flat-top. Each point represents one plasma in the NSTX database, with the entire database plotted. In the first frame the shots are sorted by year as indicated. In the second frame, the shots are sorted by elongation, indicating the correlation between the increase in achievable plasma elongation and the increase in β_t.

performance, we plot the pulse averaged β_t versus the pulse length over which the averaging was performed for the entire NSTX database in figure 5. In the first frame of the plot the data is colour sorted by year, whereas in the second frame the colour sorting is by elongation. As is apparent in the plot, the improvement in pulse average β_t is clearly correlated with the increase in plasma elongation that came along with the control system improvements for 2004.

In order to understand the role of bootstrap current in increasing the pulse averaged β, a new figure of merit is defined which is particularly relevant to the spherical torus. The parameter which will be referred to as the sustained β fraction is defined as $\beta_{sus} \equiv 0.5\sqrt{\varepsilon}\beta_p \times \beta_t \approx f_{bs} \times \beta_t$, where $\varepsilon \equiv a/R$, $\beta_p \equiv 2\mu_0\langle P\rangle/\bar{B}_p^2$ (where $\bar{B}_p$ is the poloidal magnetic field averaged over the plasma minor circumference), $f_{bs} \equiv I_{bs}/I_p$ is the bootstrap current fraction and where use has been made of the approximation $f_{bs} \approx 0.5\sqrt{\varepsilon}\beta_p$, which ignores the effect of finite collisionality and non-thermal particles. If we assume that ideal MHD instabilities limit $\beta_N < C_T$ (where C_T is the coefficient in the Troyon β limit $\beta_t = C_T I_p/[aB_t]$) then at fixed κ and B_t there is an intrinsic trade-off between the plasma current and the bootstrap fraction. Since the ideal MHD β_t limit is proportional to plasma current, there is also a trade-off between β_t and the bootstrap fraction. This β_{sus} parameter balances this trade-off and therefore more directly defines high performance in plasmas that depend on both bootstrap fraction and high β_t for viability as fusion devices. The advanced tokamak concept, which also relies upon the bootstrap current

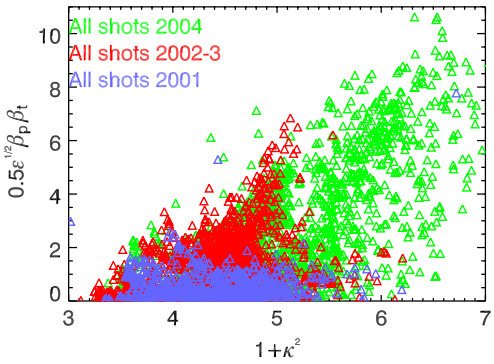

Figure 6. The parameter $0.5\sqrt{\varepsilon}\beta_p \times \beta_t$ plotted versus $1+\kappa^2$. Each point represents the pulse average of one NSTX plasma discharge, with every discharge in the NSTX database plotted.

for sustainment and high β_t, could also make use of this parameter in defining progress.

Figure 6 shows the pulse averaged value of β_{sus} for the NSTX database plotted versus the quantity $1+\kappa^2$ (one can simply show that $f_{bs} \times \beta_t \sim \beta_N^2(1+\kappa^2)$ assuming a plasma of elliptical cross-section, see, e.g. [7]). If the upper bound of β_{sus} is determined by the ideal MHD β-limit then to the degree that the elliptical approximation is adequate, plasma elongation is the only controlling variable remaining. In principle, it should also be possible to optimize β_{sus} by raising the limiting β_N through various other control techniques, but this is not the focus of this paper. It is interesting to note that the data seems to improve more rapidly with increasing elongation than is predicted by the simple model. The reason for this is apparent in figure 2. There is a partial β collapse in the lower current, lower β_t plasma before the end of the plasma current flat-top, whereas the high β phase persists until the end of the higher elongation plasma. A possible explanation for the delayed onset of instability in recent discharges is the lower plasma inductance which was correlated with the inducement of H-mode during the current ramp of the higher elongation discharge.

3. Early H-mode

The technique of inducing H-mode during the current ramp by the use of a small pause or 'flat-spot' in the current ramp combined with diverting the plasma early in the current ramp and early application of neutral beam power has been used on many different devices (see, e.g. [8]) and has recently been applied on NSTX [9]. Shown in figure 7 is a comparison between two plasma discharges, one with an induced early H-mode transition and one without. As is apparent in the figure, the flux consumption is noticeably reduced during the current ramp phase of the discharge with the early H-mode transition. (The flux consumption is proportional to the change in flux in the ohmic heating coil.) Potential reasons for the reduced flux consumption are as follows: the electron temperature profile broadens thereby reducing the plasma resistance, the pressure profile broadens increasing the bootstrap current and the broader pressure profile actually permits the achievement of higher β due to increased MHD

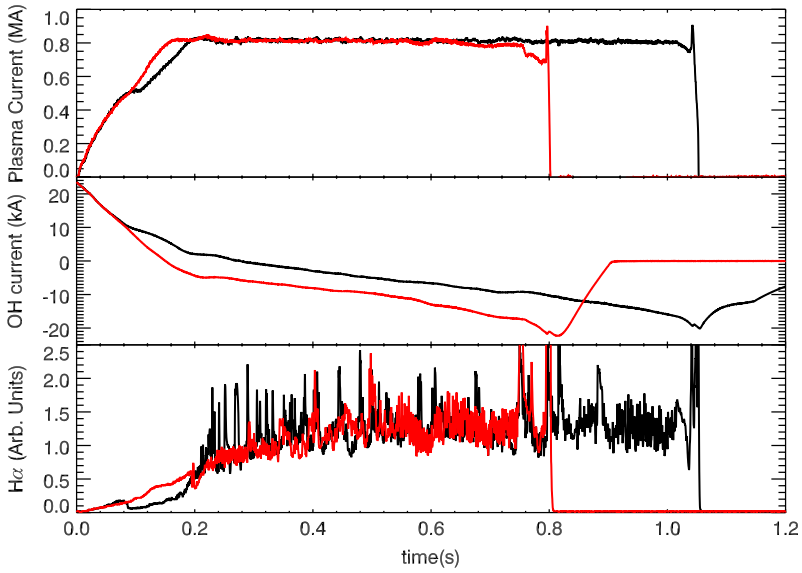

Figure 7. Figure showing the effect of the early H-mode transition on flux consumption. (*a*) Plasma current trace showing the programmed 'flat-spot' in I_p which is used to trigger the transition, (*b*) the current in the Ohmic heating coil (proportional to the flux consumed) and (*c*) the measured D_α emission showing the early H-mode (black, Shot 112546) occurs at the time of the 'flat-spot', whereas the normal H-mode transition (red, Shot 111964) is at the start of the I_p flat-top.

stability with broad pressure profiles. Detailed analysis of the relative contributions of these different effects is ongoing.

The early H-mode scenario delays the onset of deleterious MHD, which is still the primary cause of plasma termination. The limiting MHD is believed to be due to the relaxation of the residual inductively driven current into the core of the discharge. Work is ongoing to analyse the MHD stability of similar discharges using the recently commissioned motional Stark effect polarimetry diagnostic to verify understanding of the behaviour of these long pulse discharges.

4. Integrated scenario modelling

Given the experimental demonstration that plasmas with high elongation are achievable on NSTX, and that high elongation has led to an increase in the pulse averaged β_t, it is a natural step to investigate the potential for maintaining all the plasma current non-inductively in NSTX while optimizing the achievable β_t. Methods for optimizing the maximum achievable β_t with respect to ideal MHD limits have been described in the past [10] using optimized kinetic profiles. These optimizations indicated that strong plasma shaping was an important factor in achieving elevated β_t. It is also useful to use actual experimentally measured kinetic profiles as the basis for this optimization.

Recently, modelling efforts using the modelling codes TSC [11] and TRANSP [6] have identified an attractive scenario that is fully non-inductively sustained with $\beta_t \sim 40\%$ [12]. Diffusivity profiles determined from NSTX experiments by TRANSP were scaled according to the ITER98Hpby2 [13] scaling relation. This scenario incorporated calculations of EBW and beam driven current as well as bootstrap current. The modelled plasma is calculated to be stable for $n = 1$ ideal MHD modes in the presence of an ideal conducting wall. Current profiles are shown for two modelled cases

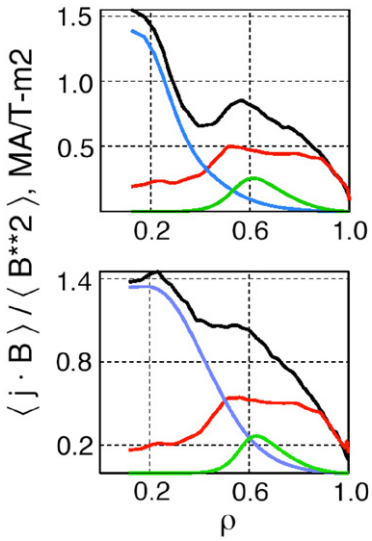

Figure 8. Parallel current density as calculated by the TSC code for 800 kA and 1.0 MA high β 100% non-inductive projected plasmas, with diffusivities based on those from discharge 109070, showing the bootstrap (red), NBCD (blue) and EBWCD (green) contributions.

(also from [12]) with 100% non-inductively driven current in figure 8.

The scenario identified requires strong plasma shaping with the simultaneous achievement of high elongation ($\kappa \sim 2.5$) and high triangularity ($\delta \sim 0.8$). Equilibrium calculations indicated that this was not possible with the original NSTX poloidal field coil set. As a result, the PF1A coils (indicated in figure 9) have been modified, in order to produce the plasma identified through modelling. Also shown in figure 9 is a comparison between a typical double-null, high-elongation shot from 2004 and a calculated equilibrium using the same plasma profiles but the modified PF1A coil set. The modified

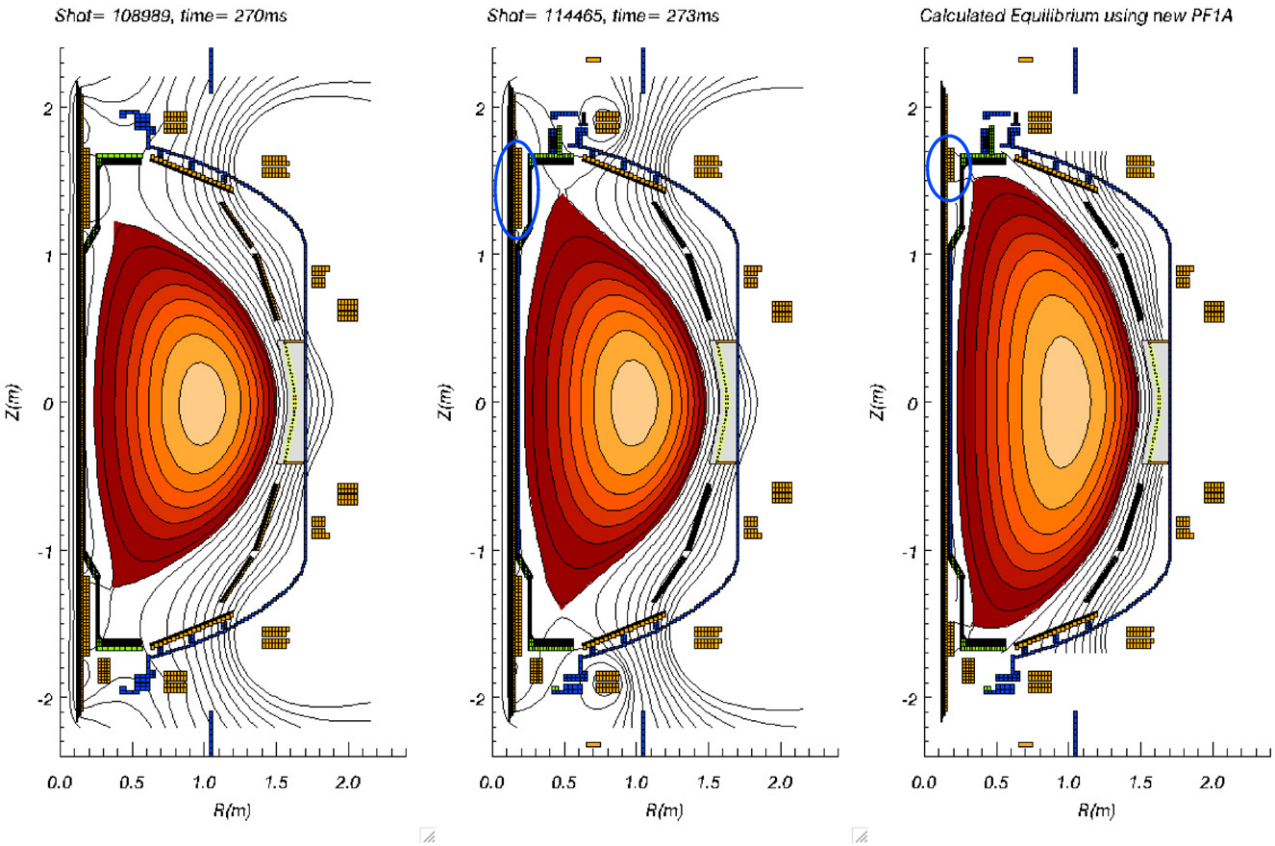

Figure 9. Evolution of the NSTX plasma shape from year to year. (*a*) High triangularity double null plasma from 2002, $\kappa = 2.0$, (*b*) moderate triangularity high elongation double null from 2004, $\kappa = 2.3$, and (*c*) a calculated high triangularity high elongation plasma which should be possible in 2005 as a result of the modification of the PF1A coil, $\kappa = 2.5$. The blue ellipses encircle the PF1A coil.

poloidal field coils will be used to investigate the behaviour of these highly shaped plasma discharges in the coming year. The modelled scenario requires a functional non-inductive current drive mechanism (e.g. which is described in the next section) to provide ∼10% of the plasma current.

5. HHFW and EBW heating and current drive

HHFW heating has been proposed as an attractive means for heating and driving current in an ST. The NSTX HHFW heating system consists of a 12 strap antenna connected to six independent RF sources [14]. The total power which has been injected by the system is 6 MW. Experiments have been performed which demonstrate that significant heating power can be deposited on the electrons and that current can be driven with directed waves. The surface voltage from two plasma discharges, one with co-phasing and one with counter, are shown in figure 10. Because the heating efficiency is observed to vary substantially between the different phasings, the total power was adjusted so that the electron temperatures match. Four different electron temperature profiles, two from each shot, are overlaid in figure 11 indicating the quality of the temperature match. The difference in loop voltage is estimated [14] to correspond to a total difference in HHFW driven current of 180 kA between the two cases (110 kA co-current, 70 kA counter). The plasma current in these discharges is 500 kA.

HHFW have been observed to damp on both edge thermal ions and fast particles injected by neutral beam heating as well as on electrons. This ion damping behaviour is an important feature of high harmonic fast wave heating that must be more fully understood to avoid undesired diversion of current drive power into bulk ion heating, thereby reducing the current drive efficiency. Work is ongoing to develop a better understanding of the physics that controls HHFW ion damping, but initial indications are that the fast ion heating is due to direct wave damping [15], whereas the edge bulk heating is due to parametric decay (i.e. a non-linear three-wave coupling which conserves momentum and energy) into an ion Bernstein mode and an ion quasi-mode [16].

Theoretical calculations have indicated that EBW may be an efficient method for heating electrons and driving current in NSTX, particularly at high β [17]. Since NSTX operates well into the over-dense regime (where $\omega_{pe} \gg \omega_{ce}$, where ω_{pe} is the electron plasma frequency and ω_{ce} the electron cyclotron frequency) conventional electron cyclotron heating is not viable. However, EBWs can propagate in such plasmas and are strongly absorbed at harmonics of the electron cyclotron frequency. Detailed numerical modelling has also indicated that these waves can be used to efficiently drive off-axis current, in keeping with the requirement indicated by integrated scenario modelling .

In order for the heating scheme to work, a conversion scheme is needed to couple power from the electromagnetic

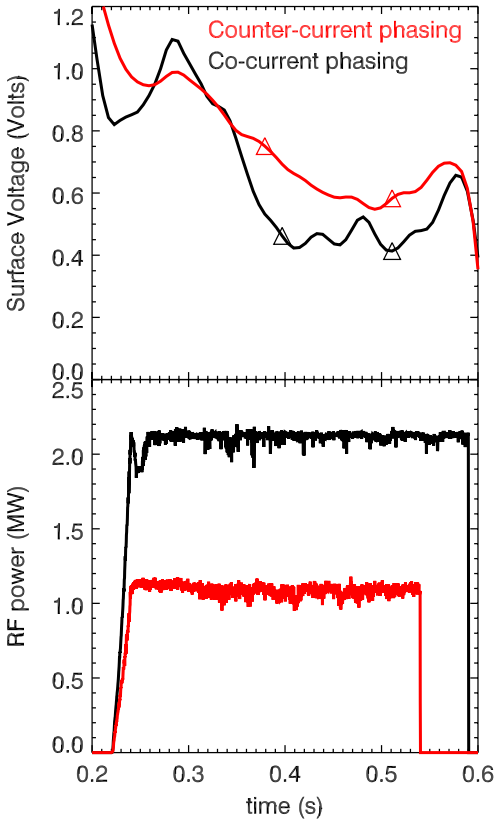

Figure 10. Results from an experiment designed to demonstrate current drive using HHFW on NSTX. The first frame shows the surface voltage for two discharges for which the direction of the launched wavefront was reversed (co-current phasing is black and counter-current phasing is red). The electron temperature profiles for the time points indicated by the triangles are shown in figure 11. Since the efficiency of heating varies substantially between co- and counter-phasing, the heating power (shown in the second frame) was adjusted until the measured electron temperatures matched.

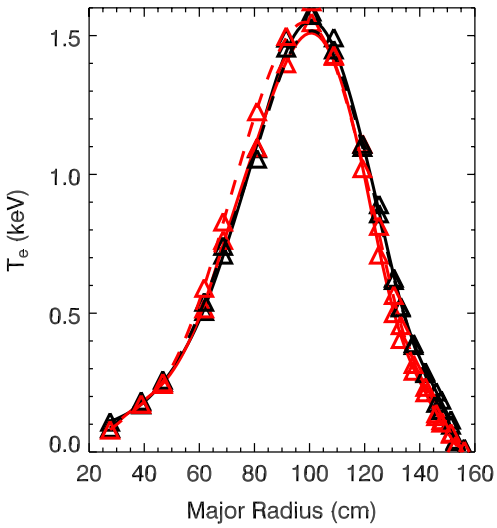

Figure 11. Comparison of the measured electron temperature profiles for two times for each discharge shown in figure 10. For each shot, the solid line is the earlier time and the dashed line is the later time.

wave launched by a microwave antenna to the electrostatic wave that is capable of propagating inside the plasma boundary. A scheme has been proposed which couples the O-mode electromagnetic wave to the Bernstein wave. Recent measurements of EBW emission support the viability of this coupling mechanism [18]. Radiometer measurements of the emitted EBW have confirmed that there is indeed efficient emission of waves in the EBW range of frequencies at the viewing angle where the coupling condition is satisfied.

6. Summary

NSTX is developing and incorporating numerous tools to simultaneously achieve high bootstrap fraction and high toroidal β. Improved control capability has already broadened the long pulse operating regime substantially, enabling 1 MA of plasma current with 1 s pulse lengths (0.8 s current flat-top). Induced early H-mode transitions have reduced plasma internal inductance which in turn has delayed the onset of pulse limiting MHD. Progress has been made on both HHFW heating and current drive and EBW emission studies. Integrated scenario modelling has identified a steady-state scenario that is stable at $\beta_t \sim 40\%$. The NSTX poloidal field coil set has been modified to enable the achievement of this scenario. The advances to date on NSTX represent significant progress towards demonstrating the viability of the ST concept for magnetic fusion.

Acknowledgment

This work was supported by the US Department of Energy Grant under contract number DE-AC02-76CH03073.

References

[1] Peng Y.-K.M. and Strickler D.J. 1986 *Nucl. Fusion* **26** 769
[2] Ono M. *et al* 2000 *Nucl. Fusion* **40** 557
[3] Gates D.A. and the NSTX national research team 2003 *Phys. Plasmas* **10** 1659
[4] Sabbagh S.A. *et al* 2001 *Nucl. Fusion* **41** 1601
[5] Lao L.L. *et al* 1985 *Nucl. Fusion* **25** 1421
[6] Hawryluk R.J. 1980 *Physics of Plasmas Close to Thermonuclear Conditions* vol 1 (Brussels: CEC)
[7] Mau T.K. *et al* 1999 *Proc. 18th IEEE/NPSS Symp. on Fusion Engineering (Albuquerque, NM, USA)* p 45
[8] Wade M.R. *et al* 2003 *Nucl. Fusion* **43** 634
[9] Menard J.E. *et al* 2005 *Nucl. Fusion* **45** 539
[10] Menard J.E., Jardin S.C., Kaye S.M., Kessel C.E. and Manickam J. 1997 *Nucl. Fusion* **37** 595
[11] Jardin S., Pomphrey N. and Delucia J. 1986 *J. Comput. Phys.* **66** 481
[12] Kessel C.E. *et al* 2005 *Nucl. Fusion* **45** 814
[13] ITER Physics Basis 1999 *Nucl. Fusion* **39** 2175
[14] Wilson J.R. *et al* 2003 *Phys. Plasmas* **10** 1733
[15] Rosenberg A.L. *et al* 2004 *Phys. Plasmas* **11** 2441
[16] Biewer T., Bell R.E., Diem S.J., Phillips C.K., Wilson J.R. and Ryan P.M. 2005 *Phys. Plasmas* **12** 056108
[17] Taylor G. *et al* 2004 *Phys. Plasmas* **11** 4733
[18] Taylor G. *et al* 2005 *Phys. Plasmas* **12** 052511